Electronic Supplementary Material (ESI) for Chemical Communications
This journal is © The Royal Society of Chemistry 2011

Electronic Supplementary Information

for

Morphology Evolution of $Cu_{2-x}S$ Nanoparticles: From Spheres to Dodecahedrons

Wenhua Li,[a] Alexey Shavel,[b] Roger Guzman,[c] Javier Rubio-Garcia,[a] Cristina Flox,[a] Jiandong Fan,[b] Doris Cadavid,[a] Maria Ibáñez,[b] Jordi Arbiol,[c,d] Joan Ramon Morante[a,b] and Andreu Cabot*[,a,b]

a Catalonia Institute for Energy Research, IREC, Jardí de les Dones de Negre, 1, Planta 2, 08930, Sant Adrià del Besós, Barcelona, Spain. Fax: 34933563802; Tel: 34933562615; E-mail: acabot@irec.cat

b Departament Electronica, Universitat de Barcelona, Barcelona, 08028, Spain.

c Institut de Ciencia de Materials de Barcelona, CSIC, Campus de la UAB, Bellaterra, 08193, Spain.

d Institució Catalana de Recerca i Estudis Avançats, ICREA, Barcelona, 08010, Spain.

Synthesis conditions

Figure	$CuCl_2 \cdot 2H_2O$ (mmol)	TBDS (mmol)	Oleylamine (g)	Dodecanethiol (mmol)	Reaction T (ºC)	Reaction time (min)
1a	0.5	5	10	5	220	10
1b	0.5	10	12	0	180	40
1c	0.5	10	12	0	190	60
1d	0.5	10	12	0	180	40
2a-c	1	10	12	0	200	40-60
2d-f	2	10	12	0	200	40-60
3a	2	10	12	0	200	60
3b	5	50	100	0	180	40
3c	5	10	12	0	200	60
3d	5	10	12	0	200	60
3e	8	10	12	0	200	40
3f	8	10	12	0	200	60

$Cu_{2-x}S$ nanoparticles were obtained from the reaction of copper chloride with di-tert-butyl disulfide (TBDS) inside a heated oleylamine solution (OLA). In a typical preparation, 0.0852 g of $CuCl_2 \cdot 2H_2O$ (0.5 mmol, 99.99%, Aldrich) and 12 g of OLA (70%, Aldrich) were introduced inside a four-neck flask and heated to 200ºC under an argon flow. The yellowish transparent solution produced was maintained at 200 ºC for one additional hour for purification, i.e. to remove oxygen, water and other low-boiling point impurities. Afterwards, the temperature was set to 180 ºC and 1 ml TBDS (5 mmol, 97%, Aldrich) was

This journal is © The Royal Society of Chemistry 2011

injected through a septum. The mixture was maintained at the reaction temperature for up to 1 hour to allow the nanoparticles growth. Then, the flask was rapidly cooled down to room temperature.

The nanoparticles were washed by multiple precipitation and dispersion steps using toluene as a solvent and ethanol as the precipitating agent. The reported synthesis procedure, characterized by a low nucleation rate, produced highly monodisperse nanocrystals, thus not requiring any size selection process. For TEM and SEM characterization, drops of solution containing the nanoparticles were dried on carbon-coated copper grids and silicon substrates, respectively. The high monodispersity of the particles leaded to their self-assembly upon solvent removal.

This journal is © The Royal Society of Chemistry 2011

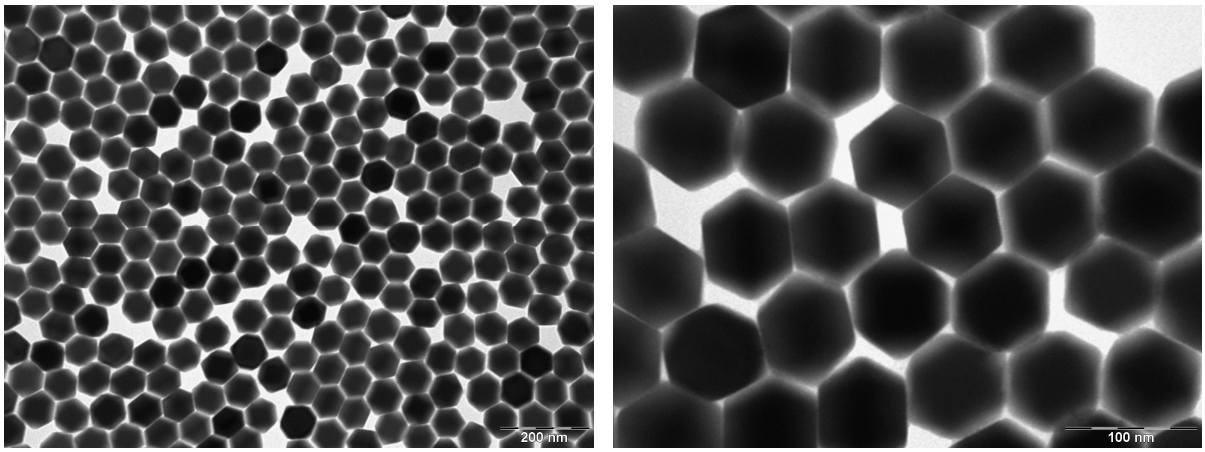

Fig. S1 TEM images of tetradecahedral nanocrystals obtained in the same synthesis conditions as in figure 3a.

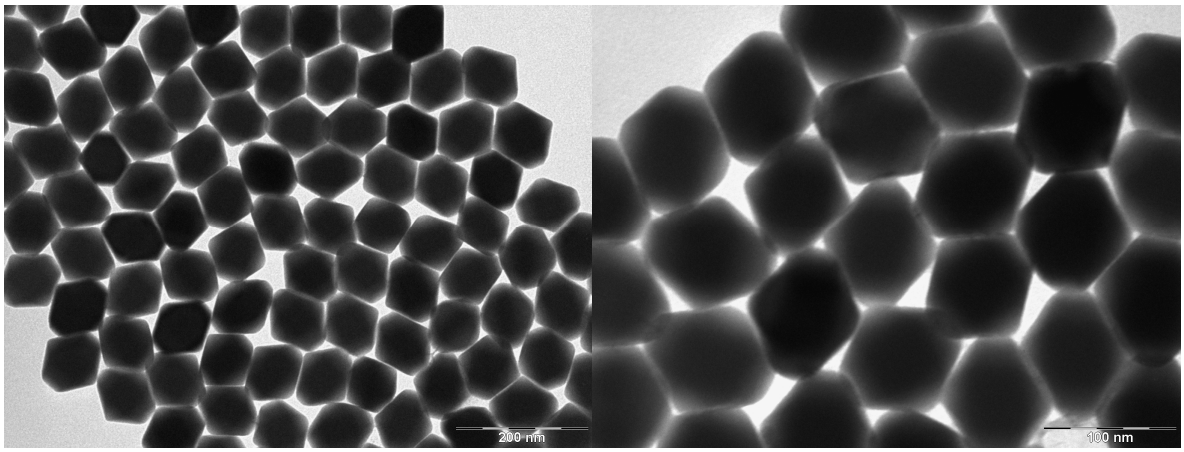

Fig. S2 TEM images of tetradecahedral nanocrystals obtained in the same synthesis conditions as in figure 3c.

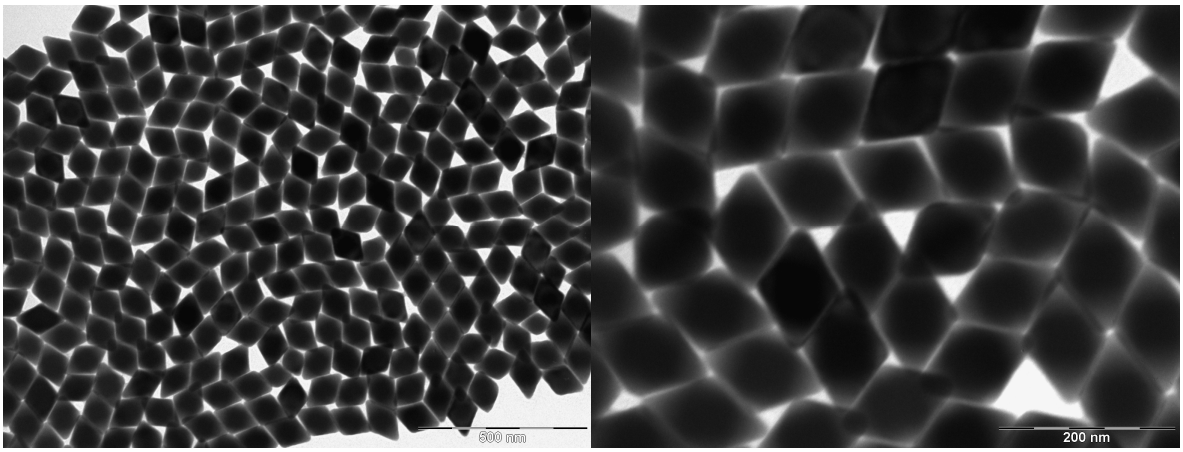

Fig. S3 TEM images of dodecahedral nanocrystals obtained in the same synthesis conditions as in figure 3e.

This journal is © The Royal Society of Chemistry 2011

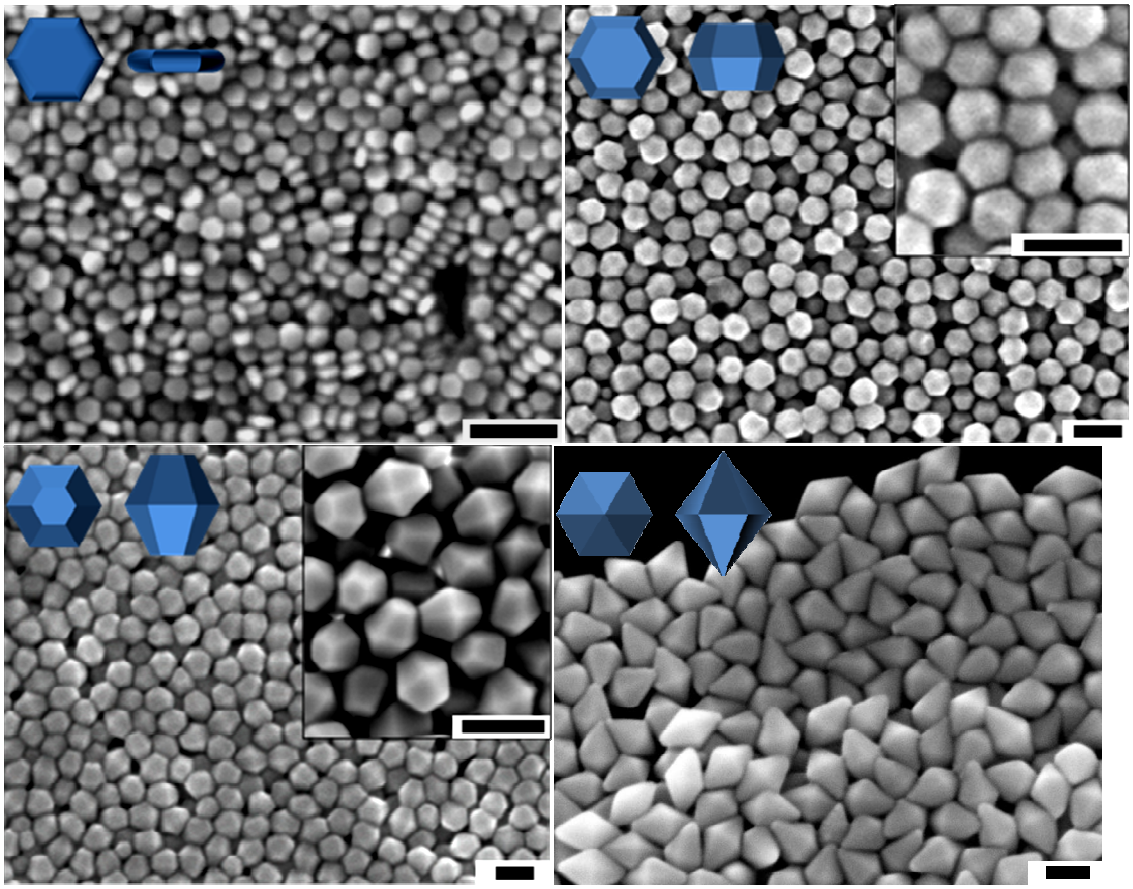

Fig. S4 SEM images of nanodisks, tetradecahedral and dodecahedral nanocrystals obtained in the same synthesis conditions as in figure 1d, 3a, 3c and 3e, respectively. Scale bars correspond to 100nm.

.

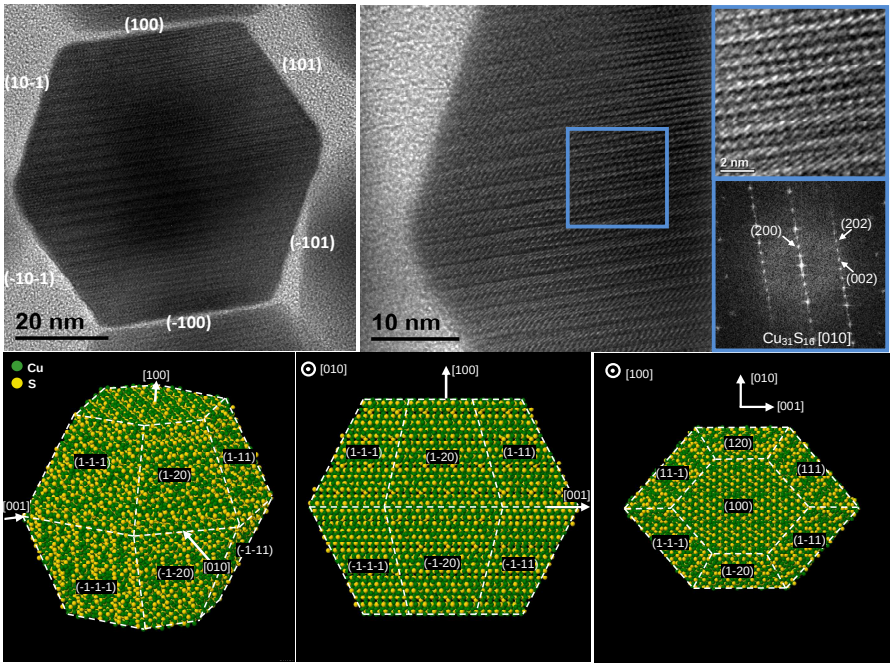

Fig. S5 HRTEM image (a) and details (b,c) of a $Cu_{1.96}S$ tetradecahedron, with power spectrum structure analysis (d), and corresponding scaled (1:5) 3D atomic model in perspective (e), frontal (f) and top (g) views.

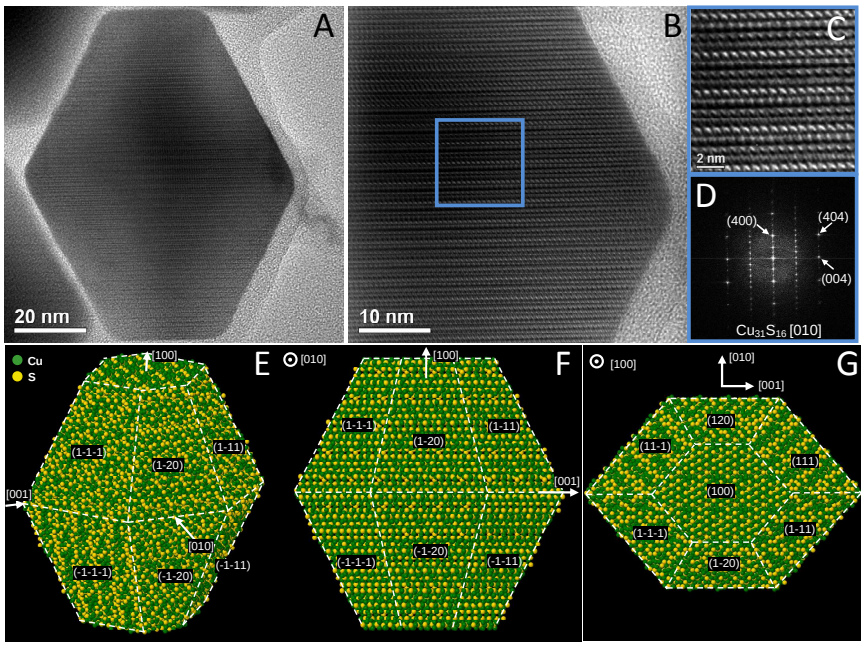

Fig. S6 HRTEM image (a) and details (b,c) of a $Cu_{1.96}S$ tetradecahedron, with power spectrum structure analysis (d), and corresponding scaled (1:5) 3D atomic model in perspective (e), frontal (f) and top (g) views.

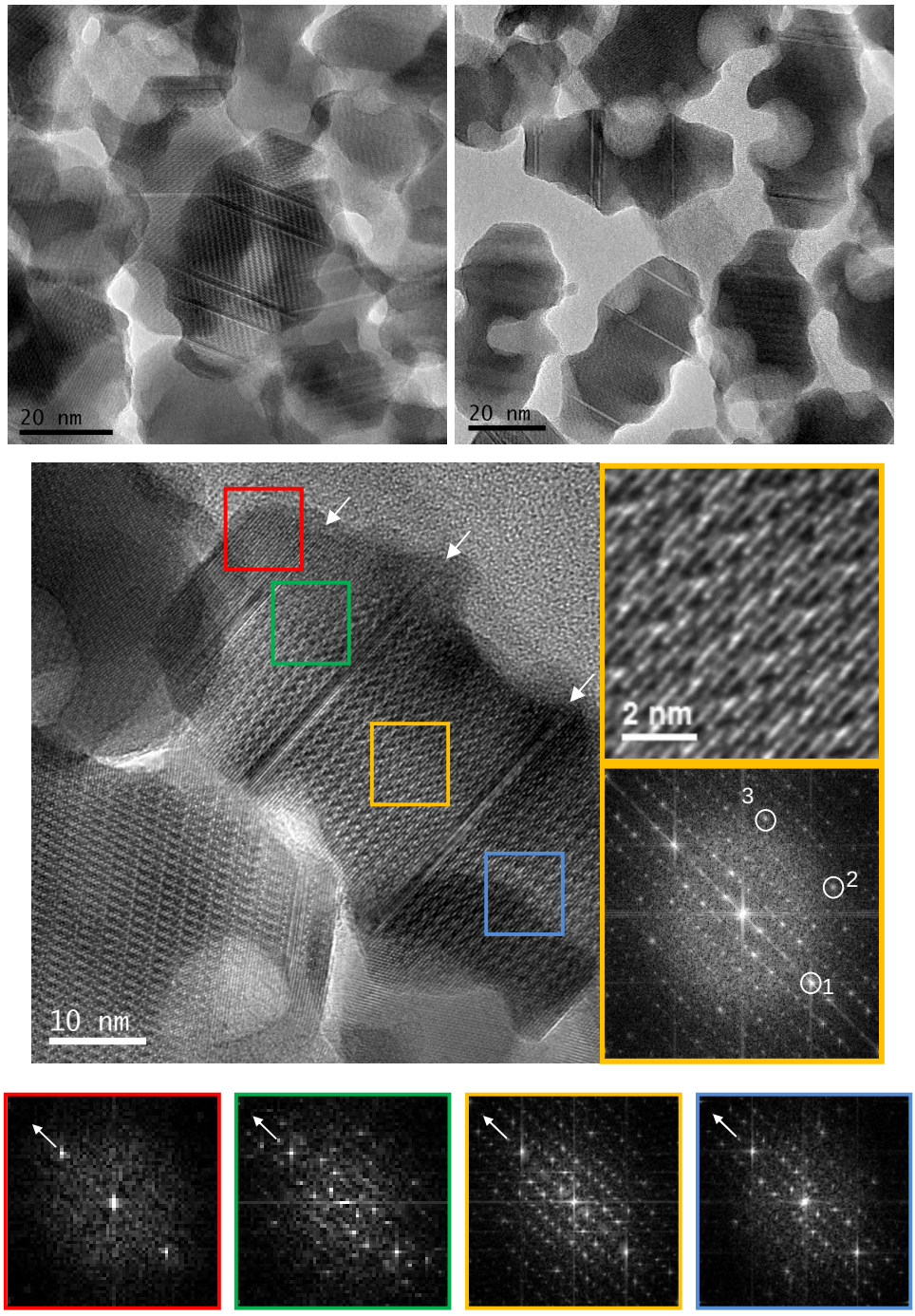

Fig. S7 HRTEM images of the nanoparticles obtained from the assembly of thin nanoplates at the early stages of formation of $Cu_{2-x}S$ tetrahedrons. Some holes were created during an oxygen plasma treatment applied to clean the samples from organics. From the HRTEM images it is clearly seen how the particles are composed of multiple crystals in perfect epitaxy but clearly separated by junctions or planar defects (white arrows in the image). As revealed by the FFTs of each respective crystal, no disorientation is appreciated respect to the common longitudinal axis.

This journal is © The Royal Society of Chemistry 2011

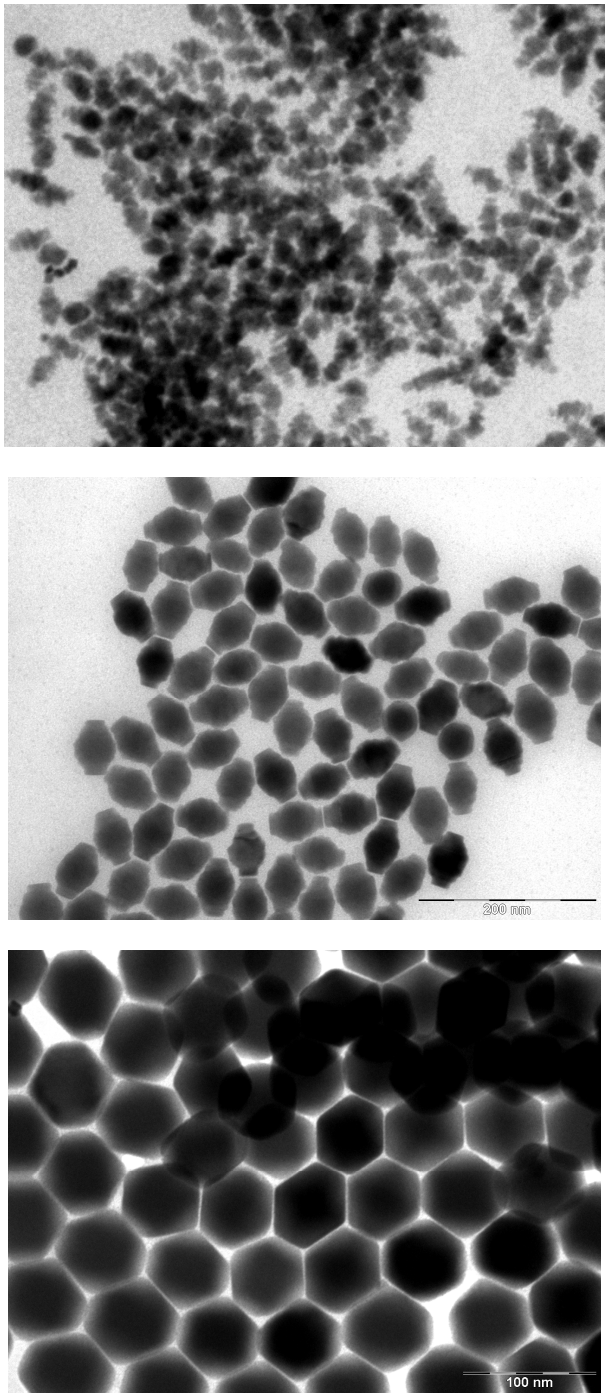

Fig. S8. TEM images of the particles obtained at the different stages during the formation of $Cu_{2-x}S$ tetradecahedrons. Same synthesis conditions as in figure 3c.

This journal is © The Royal Society of Chemistry 2011

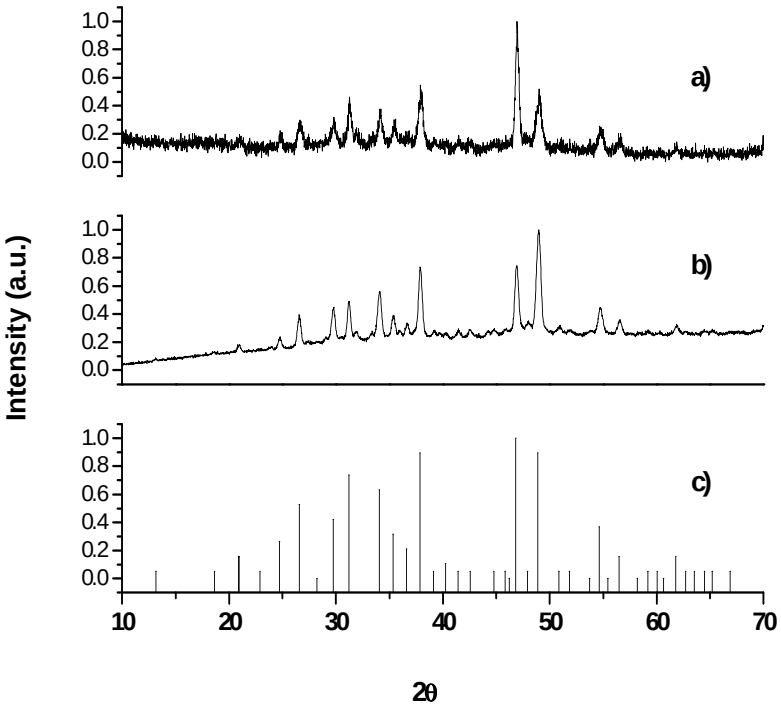

Fig. S9. XRD pattern of the nanodisks synthesized at a) 180ºC, 40min and b) 200ºC, 20min. c) Reference pattern corresponding to monoclinic roxbyite (JCPDS no. 23-958)

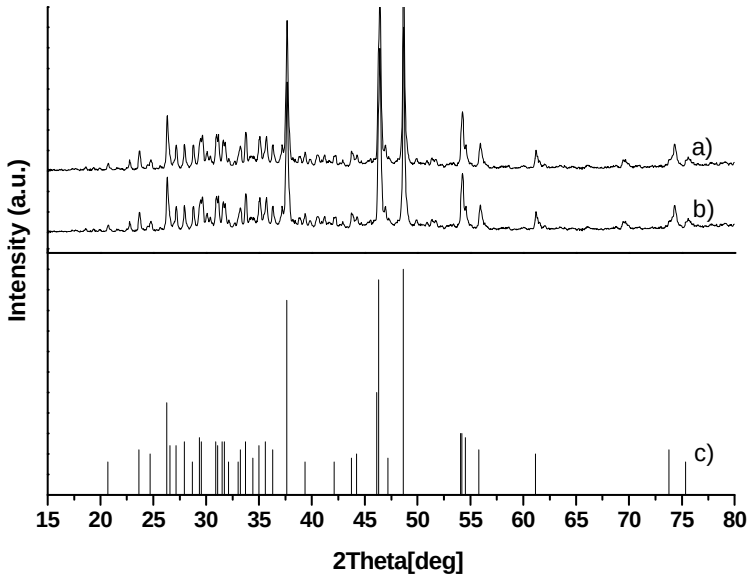

Fig. S10. XRD pattern of the tetradecahedrons obtained in the synthesis conditions of figure 3e (a) and 3c (b). c) Reference pattern corresponding to the monoclinic Djurleite (JCPDS no. 23-959)

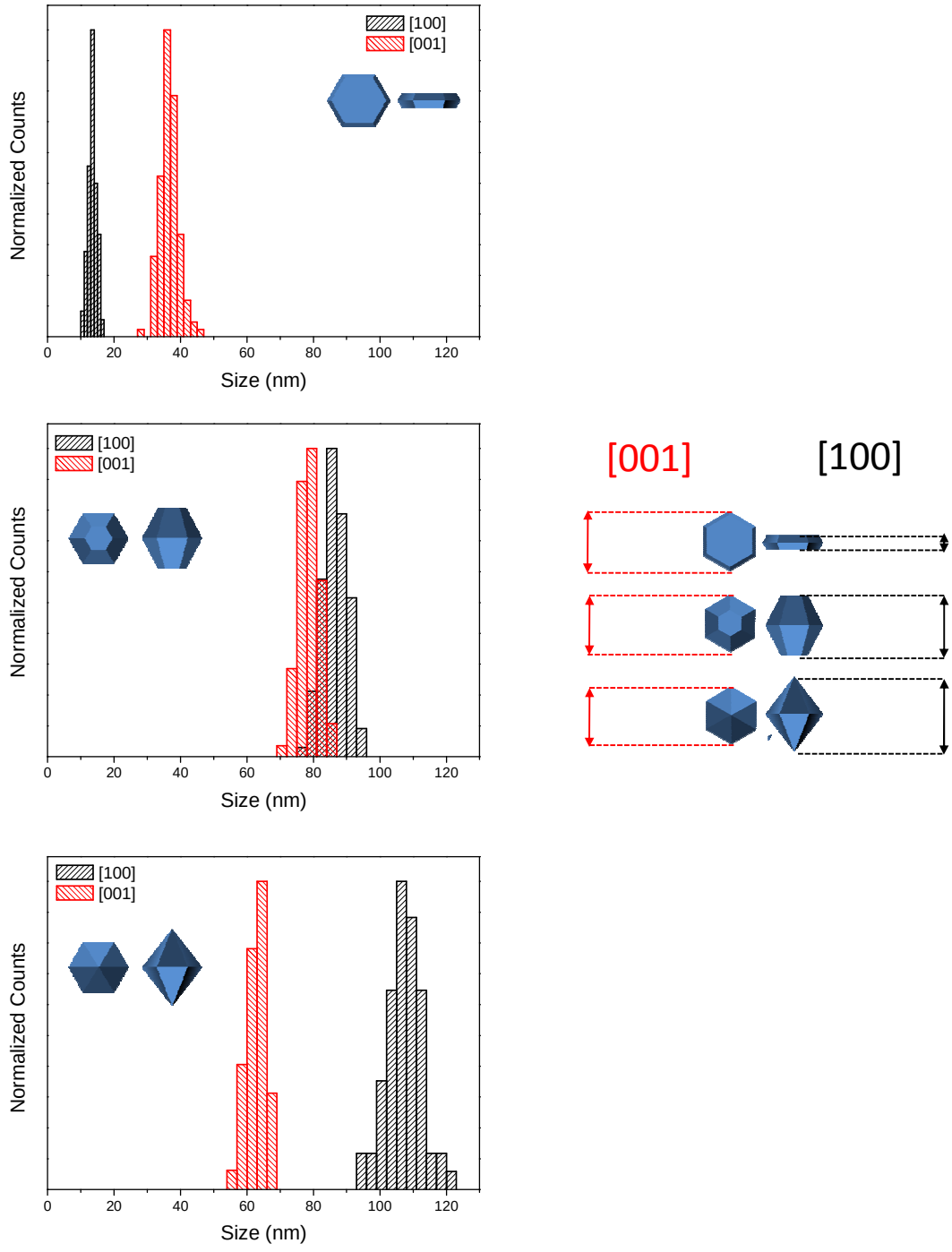

Fig. S11. Histograms showing the typically-obtained nanocrystal size distributions. In black, the size in the [100] crystal direction corresponds with that in the axial direction. That is the disk thickness and the long dodecahedron dimension. In red, the size in the [001] crystal direction corresponds to the disk diameter and to the short dimension of the dodecahedral particles. Top, middle and bottom histograms correspond to nanodisks, tetradecahedral nanocrystals and dodecahedrons, respectively.

Electronic Supplementary Material (ESI) for Chemical Communications
This journal is © The Royal Society of Chemistry 2011

Test of $Cu_{2-x}S$ nanocrystals as cathodes in all-vanadium redox flow batteries (VRB).

Due to their flexibility and fast response, flow batteries are one of the most promising solutions for load leveling and peak shaving of renewable energies such as solar and wind.[1] In a flow battery, the energy is chemically stored in two independent solutions containing each of them a redox couple. Unlike in other energy storing devices, such as Li-ion batteries or electrochemical capacitors, in the redox battery, energetic capacity and power are independent. Among redox batteries, better performances in terms of life time and cost are obtained when using solutions of vanadium ions for both semi-reactions: $[VO]^{2+}/[VO_2]^{+}$, positive cell; and V^{3+}/V^{2+}, negative cell. In this case, the battery is known as an all-vanadium redox flow battery (VRB).

Carbon-based electrodes, such as graphite felts,[3] carbon nanotubes,[4] carbon fibers[5] or mesoporous carbon[6] are typically used in VRB because of their relative low cost, high surface area, chemical stability and good electrical conductivity. However, their kinetic reversibility is rather poor, which is especially critical at the cathode. The efficiency of VRB is usually limited by the rate and potential of the $[VO]^{2+}/[VO_2]^{+}$ cathodic reaction.[2] Thus, the introduction of catalytic elements to improve the efficiency of these reactions has been widely studied.[6]

$Cu_{2-x}S$ nanocrystals were thoroughly purified by multiple precipitation and redisperion cycles. Subsequently, 1 mg of nanoparticles was supported on 1 cm^2 planar graphite substrate by drop casting. The remaining organic ligands were removed using an aqueous solution of hydrazine. Then, the material was dried in vacuum at 100ºC. Afterwards, the supported particles were covered by a solution of Nafion (10 %) in water. Upon evaporation of the solvent, the electrochemical activity was characterized by means of cyclic voltametry using a Biologic VMP-3 potentiostat linked to a 50 mL glass thermostated electrochemical cell. The cell was equipped with a platinum counter electrode and a Luggin capilar $Hg/Hg_2SO_4/K_2SO_4$ (sat) reference electrode. The VRB cathode was used as a working electrode. Measurements were performed in an inert atmosphere using 30 mL of a 0.5 M $VOSO_4$ and 1 M H_2SO_4 solution.

The electrocatalytic activity (peak currents and potentials of redox reactions) and the reversibility of the cathodic reaction $[VO]^{2+}/[VO_2]^{+}$ are the key parameters to evaluate an electrode performance in redox flow batteries. In particular, the energy storage efficiency of a battery is proportional to the ratio of its discharge and charge voltages.[2] The lower the oxidation potential, the lower the voltage needed to charge the battery, and thus the higher its efficiency.

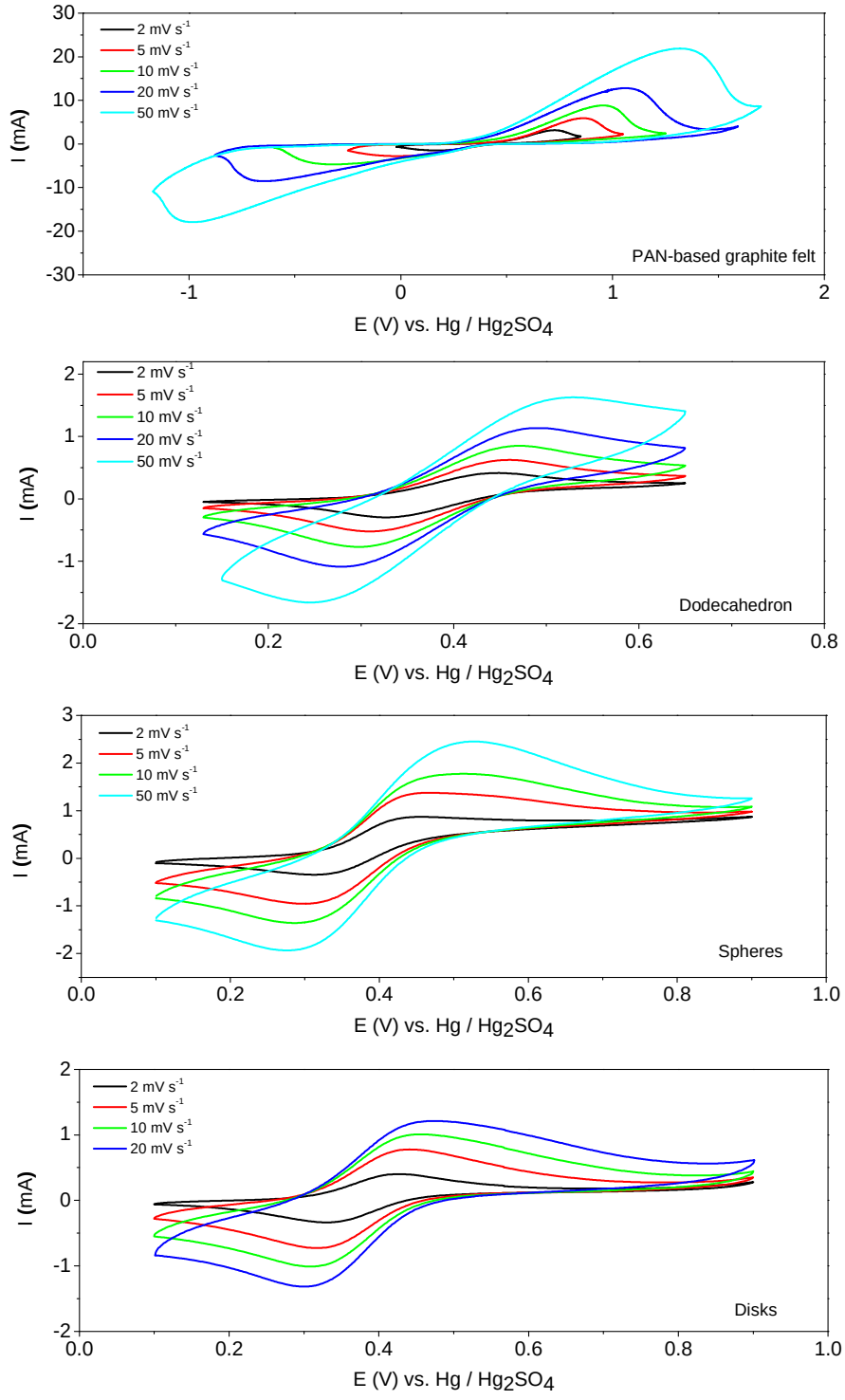

Figure S12. Cyclic voltammograms at different scan rates obtained using the PAN-based graphite felt (top) and the different $Cu_{2-x}S$ nanocrystal morphologies supported on a planar graphite substrate (as indicated on each graph).

This journal is © The Royal Society of Chemistry 2011

In figure S12, the voltammograms obtained from electrodes containing $Cu_{2-x}S$ nanoparticles with different morphologies are compared with those of a polyacrylonitrile (PAN) -derived graphite felt. Notice how the voltage difference between the peaks corresponding to the reduction and oxidation events and its dependence with the scan rate are much lower for the electrodes containing $Cu_{2-x}S$ nanocrystals than for the naked graphite. In figure S13, the voltage of the reduction and oxidation peaks obtained with the different nanocrystal geometries is plotted as a function of the scan rate. No clear differences in the oxidation and reduction potentials were obtained between the different nanocrystal geometries, pointing towards the existence of similar reaction mechanisms.

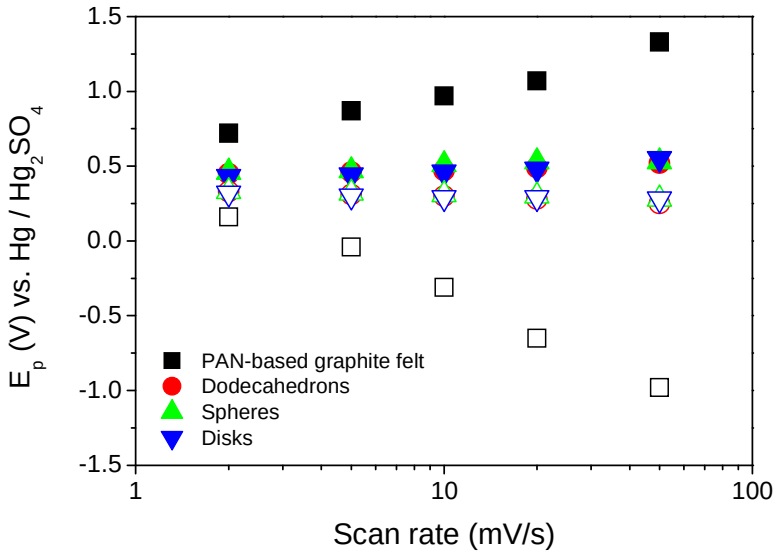

Figure S13. Voltage of the cathodic and anionic peaks as a funcion of the scan rate obtained from the different nanocrystal morphologies and the PAN-based graphite felt.

Figure S14 shows the anodic vs. cathodic current ratio as a function of the scanning rate. In a reversible process, the ratio between the current intensities of the anodic and cathodic peaks should be close to 1.[7] Notice how electrodes containing $Cu_{2-x}S$ nanocrystals usually showed better reversibilities than naked graphite electrodes.

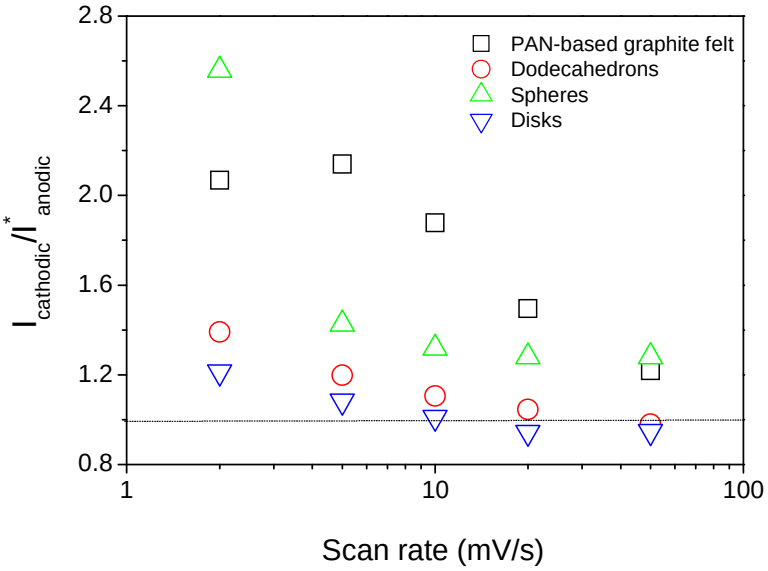

Figure S14. Anodic vs. cathodic peak current ratio obtained with the different nanocrystal morphologies and the PAN-based graphite felt.

Furthermore, in a reversible process, the forward scan peak current should be proportional to the square root of the scan rate.[7] Figure S15 shows the dependence of the current with the square root of the scan rate. Lineal dependences were obtained for all electrodes containing $Cu_{2-x}S$ nanocrystals, which pointed towards a vanadium-diffusion limited mechanism. In this regime, the Randles-Sevcik equation can be used to determine the apparent diffusion coefficients of the vanadium species in the electrodes:

$$i_p = 2.686 \times 10^5 n^{3/2} A D^{1/2} C v^{1/2}$$

where i_p is the peak current, n the number of electrons transferred in the redox reaction, A is the electrode area, D the diffusion coefficient, C the concentration of vanadium in solution and v the scan rate. Among the different morphologies, the highest diffusion coefficients were obtained with the electrodes containing $Cu_{2-x}S$ dodecahedral nanocrystals: 2×10^{-8} cm^2 s^{-1}. Nevertheless, no conclusive differences in the performance of the distinct morphologies can be obtained from these preliminary measurements.

The limited current intensities and the associated low diffusion coefficients obtained were related to the presence of the Nafion layer and the small surface area of the electrodes containing $Cu_{2-x}S$ nanocrystals. The Nafion layer was required to prevent the degradation of the $Cu_{2-x}S$ nanocrystals. However, its thickness needs to be optimized to maximize the current density. On the other hand, the use of 3D porous graphite supports will highly increase the nanocrystal dispersion and maximizing the number of reaction sites accessible for the vanadium

species. In this sense, notice that the porous 1 cm^3 graphite felt used here for comparison had a surface area between 2 and 3 orders of magnitude larger than the planar graphite electrode, which could account for a 100-1000 fold increase in the current intensity. Another parameter which will need optimization when using 3D electrode supports is the density of $Cu_{2-x}S$ nanocrystals. Too high densities could led to saturation of the surface and thus to poorer electrochemical performance. Also the surface dispersion of the nanoparticles needs to be optimized and their aggregation prevented. This may be especially important and challenging for $Cu_{2-x}S$ nanodisks, which tend to stack face to face.

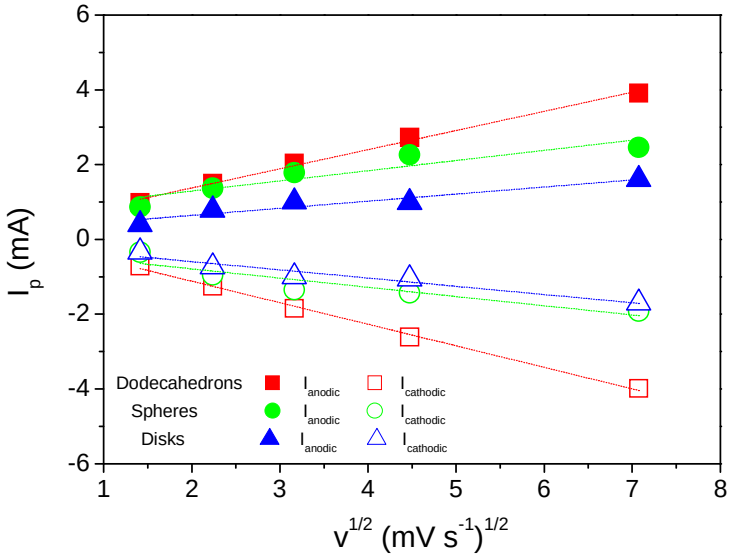

Figure S15. Current at the redox peaks as a function of the square root of the scan rate

In conclusion, the presence of $Cu_{2-x}S$ nanocrystals significantly reduced the reduction potentials and increased the reversibility of the process. We believe the present work to provide the basics for developing more efficient VRB using $Cu_{2-x}S$ nanocrystals as catalyst in the cathodes.

This journal is © The Royal Society of Chemistry 2011

References

1. (a) Huang, K. L.; Li, X. G.; Liu, S. Q.; Tan, N.; Chen, L. Q., *Renew. Energ.* **2008,** *33*, 186; (b) Fabjan, C.; Garche, J.; Harrer, B.; Jorissen, L.; Kolbeck, C.; Philippi, F.; Tomazic, G.; Wagner, F., *Electrochim. Acta* **2001,** *47*, 825; (c) Skyllaskazacos, M.; Rychcik, M.; Robins, R. G.; Fane, A. G.; Green, M. A., *J. Electrochem. Soc.* **1986,** *133*, 1057.
2. Ponce de Leon, C.; Frias-Ferrer, A.; Gonzalez-Garcia, J.; Szanto, D. A.; Walsh, F. C., *J. Power Sources* **2006**, *160*, 716.
3. Zhong, S.; Padeste, c.; Kazacos, M.; Skyllas-Kazacos, M. *J. Power Sources* **1993,** *45*, 29.
4. Zhu, H. Q.; Zhang., Y. M.; Yue, L.; Li, W.S.; Li, G. L.; Shu, D.; Chen, H.Y. *J. Power Sources* **2008,** *184*, 637.
5. Sun, B.; Skyllas-Kazacos, M., *Electrochim. Acta* **1991,** *36,* 513.
6. Shao, Y.; Wang, X.; Engelhard, M.; Wang, C.; Dai, S.; Liu, J.; Yang, Z.; Lin, Y. *J. Power Sources* **2010,** *195*, 4375.
7. Gosser, D. K. Jr. (Ed), Cyclic Voltammetry, VCH Publishers, **1993**.